Laboratory study on periodic heat exchanges between water and sediment in extremely shallow flows

S. López[1], A. de la Fuente[1], F. Suárez[2] and C. Meruane[1 3]

[1]Departamento de Ingeniería Civil, Universidad de Chile
[2]Departamento de Ingeniería Hidráulica y Ambiental, Pontificia Universidad Católica de Chile
[3]Modelación Ambiental SpA

Abstract

Extremely shallow lakes are found in the Altiplano, or high plain, of South America, in which large diurnal temperature variation occurs. In these shallow systems, the water temperature is control by head exchanges with the atmosphere and with the bottom sediments. As a consequence, the amplitude of the daily fluctuations in water temperature is reduced by heat exchanges with the bottom sediments. This paper describes a study of the thermal amplitudes in the water column as a function of of two dimensionless numbers, named Π_1 and Π_2. These dimensionless numbers include the thermal properties of water and sediments, besides the properties of the atmospheric source. Two experimental setups were constructed and used in order to obtain the water temperature times series, and the thickness of the diffusive sublayer.

1 Introduction

Extremely shallow lakes of a few centimeter depths are found in the Altiplano (or high plain) of the Andes mountain range in South America. These shallow lakes are located in the desert at about 3500 masl, thus supporting the life of a unique ecosystem. Previous studies conducted in these shallow lakes showed that water temperature varies from 20 to 30 °C in a day, while the air temperature varies from 0 to 30 °C in a day, and that the bottom sediments of the shallow lakes act as a heat reservoir that retains heat during the day and releases it during the night (de A. de la Fuente. Niño, 2010). As a consequence, the amplitude of water temperature fluctuation in a day is reduced by heat exchanges with the bottom sediments (de la Fuente, 2014). In this case, the heat flux from the sediments toward the water column creates unstable conditions in the shallow lakes and controls heat exchanges at the water-sediment interfaces, whereas stratified conditions are expected to occur when the heat flows from the water toward the sediment. The aim of this article is to study periodic heat exchanges across the water-sediment interface (WSI) based on the combination of laboratory experiments and numerical simulations.

Numerical simulations were based in a spectral formulation as follows. As the external forcing is periodic, water temperature can also be assumed periodic, thus enabling us to write the water temperature as the superposition of periodic functions. Consequently, the sediment temperature can be described by the second problem of Stokes. Following this spectral formulation of the solution (de la Fuente and Meruane, 2016), the dimensionless number $\Pi_1 = \kappa_s(\rho c_p)_s \alpha/(\rho c_p)_w \omega h$ quantifies the influence of sediments in the heat budget of water. (ρc_p) denotes the heat capacity of the water or the sediments, h the water depth, ω the frequency, κ_s the heat diffusion coefficient in the sediments, and $\alpha = \sqrt{\omega/2/\kappa_s}$ the sediment diffusion length of the problem. The limit $\Pi_1 \to 0$ represents the case when there is no heat storage in the sediments, while $\Pi_1 \to \infty$ represents the case when there is not

heat storage in the water column, and sediments capture/release the entire heat exchanges with the atmosphere. A second dimensionless number can be obtained from the spectral formulation of the solutions,$\Pi_2 = k_t/\omega h$, where k_t denotes the heat transfer velocity at the water-sediment interface. In this way, k_t quantifies the influence of turbulence on the heat fluxes across the WSI.

Laboratory experiments were conducted in a rectangular tank that contains sediments collected from an artificial lake near the university campus, and a water column of variable height was used in these experiments. Artificial lights were mounted above the water, and were periodically turned on and off to emulate the diurnal cycle. Time series of water temperature were recorded with a WTW standard sensor of conductivity and temperature, while time series of vertical profiles in soil were recorded with a Unisense TP-200 sensor. A second set of data were obtained using a distributed temperature sensing (DTS) system that allows obtaining the temporal evolution of vertical profiles of air, water and soil temperature simultaneously (Suárez et al., 2011).

2 Methods

2.1 Equations

To obtain the water temperature T_w in a water column with a h height, is necessary to solve the heat balance that considers heat exchanges with the atmosphere and sediments. Without considering horizontal advection and diffusion, the vertically averaged heat equation can be written as

$$(\rho c_p)_w h \frac{\partial T_w}{\partial t} = H + H_g \tag{1}$$

where $(\rho c_p)_w \approx 4.4 \times 10^6\,[J/m^{3\circ}K]$ is the water heat capacity; $H\,[W/m^2]$ is the heat flux exchanged between the water body and the atmosphere, such that when $H > 0$ the flux goes from the last mentioned to water (Bogan et al., 2003); and $H_g\,[W/m^2]$ represents the heat flux through the water-sediments interface (WSI).

Considering that the WSI has 2 sides and a coordinate system with its origin at the interface and positive numbers up, H_g can be written in two ways. On the sediments side of the WSI, H_g takes the form

$$H_g = -\,\kappa_s (\rho c_p)_s \left.\frac{\partial T_s}{\partial z}\right|_{z=0} \tag{2}$$

were κ_s can vary between 0.01 and $0.11\,[m^2/d]$; $(\rho c_p)_s$ fluctuates between 1.4 and $3.8 \times 10^6\,[J/m^{3\circ}K]$ (Fang and Stefan, 1998); and T_s represent the sediments temperature, which can be obtained by solving the heat equation in this part of the WSI, considering a impermanent problem with vertical diffusion and no advection. On the other hand, at the water side of the WSI, the heat flux through the WSI can be written as

$$H_g = -k_t (\rho c_p) w (T_w - T_{WSI}) \tag{3}$$

where T_{WSI} representes the temperature at the WSI; and $k_t\,[m/s]$ represents the heat transfer coefficient that depends of the convective heat fluxes when the temperature at the WSI is greater than the water temperature (Necati, 1977). This value was estimated using the expression

$$k_t = \frac{\kappa_s}{\delta_c} \tag{4}$$

where $\delta_c\,[m]$ represents the height of the thermal diffusive sublayer.

An analytical solution for the problem can be obtained considering the periodic properties of T_w, H and T_{WSI}. Writing these variables as a Fourier expansion of $2N+1$ terms, it can be obtained:

$$H(t) = \sum_{m=-N}^{m=N} H_m e^{iw_m t} \tag{5}$$

$$T_w(t) = \sum_{m=-N}^{m=N} T_{w_m} e^{iw_m t} \tag{6}$$

$$T_{WSI}(t) = \sum_{m=-N}^{m=N} T_{WSI_m}\, e^{iw_m t} \tag{7}$$

The temperature at the WSI is the boundary condition for the heat equation in the sediments, so, the sediment temperature can also be represented as a Fourier expansion such that each one of them is solution of the second problem of Stockes(Bachelor, 1967). In this way, the sediment temperature can be written as

$$T_s(t,z) = \sum_{m=-N}^{m=N} T_{s_m} e^{iw_m t} e^{(1+\frac{m}{|m|}i)\alpha_m\, z} \tag{8}$$

where $\alpha_m = \sqrt{|w_m|/2\kappa_s}$ and $i = \sqrt{-1}$.

When the turbulent transport at the water column is very efficient ($k_t \gg 1$), it can be assumed that $T_{w_m} = T_{WSI_m}$, so using (1), (2) and (5) the solution for the dimensionless water temperature is:

$$\frac{T_{w_m}}{\widetilde{T_{w_m}}} = \frac{1}{i + (1+\frac{m}{|m|}i)\Pi_1} \tag{9}$$

where $\widetilde{T_{w_m}} = H_m/(\rho c_p)_w\, w_m\, h$ and $\Pi_1 = \kappa_s(\rho c_p)_s \alpha_m/(\rho c_p)_w w_m h$. On the other hand, when the turbulent transport is not efficient ($T_{w_m} \neq T_{WSI_m}$), the solutions for the dimensionless water and WSI temperatures are:

$$\frac{T_{WSI_m}}{\widetilde{T_{w_m}}} = \frac{\Pi_2}{\Pi_2 + (1+\frac{m}{|m|}i)\Pi_1} \frac{T_{w_m}}{\widetilde{T_{w_m}}} \tag{10}$$

$$\frac{T_{w_m}}{\widetilde{T_{w_m}}} = \left(i + \Pi_2 \left(1 - \frac{\Pi_2}{\Pi_2 + (1+\frac{m}{|m|}i)\Pi_1} \right) \right)^{-1} \tag{11}$$

where $\Pi_2 = k_t/w_m\, h$.

2.2 Experimental setup

To measure heat fluxes at the WSI, a series of experiments were conducted in the Francisco Javier Dominguez laboratory of the Universidad de Chile, using two different experimental setups. In the first experimental setup, a rectangular recipient was used. The recipient was insulated with a 1 cm thick polystyrene layer, leaving a workspace of 10 cm height, with a base of 15.5 x $4.5 cm^2$. This recipient was filled with $5\,cm$ of organic soil of an artificial shallow lake located near to the university campus, and with a water column of $4-5\,cm$. Over the recipient, at a distance of $40\,cm$, a set of four halogen lights were mounted, each with a power of $150\,W$. In this way, approximately $500\,W$ resulted in a direct net heat source to the system. This arrangement was adjusted to turned on and off periodically so that the period of both states were the same. The tested periods were 1,2,4 y 8 hours.

On the other hand, the water temperature were recorded using a WTW standard sensor to measure conductivity and temperature, while in the WSI were measured with a micro electrode Unisense TP-200 type, which were left continuously measuring during the experiments. These sensors, at its thinnest part, have a diameter of $200\,\mu m$, so its measurement can be effectively associated with the WSI interface.

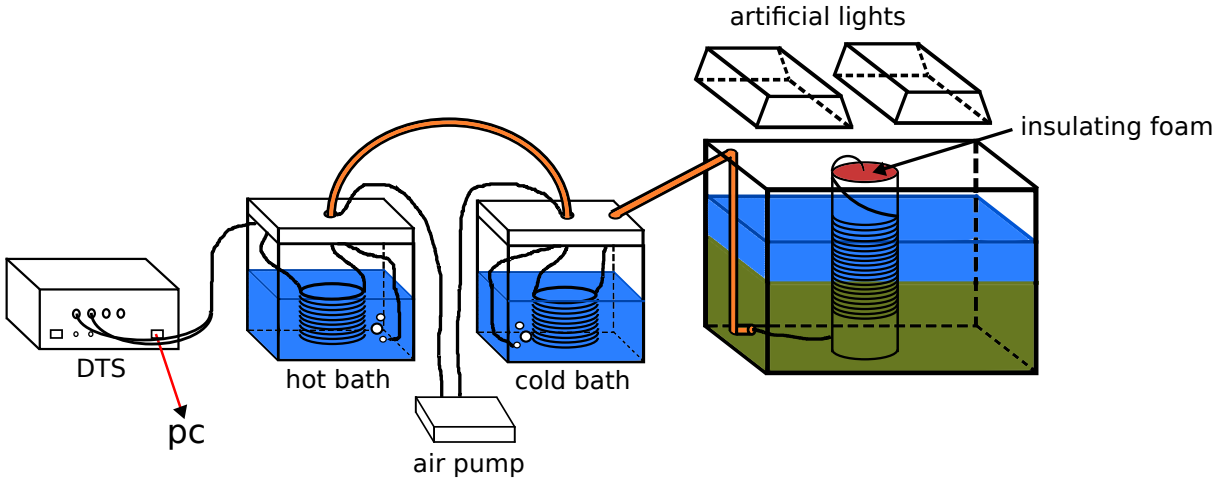

Figure 1: Diagram of DTS installation.

The second experimental setup consists in a plexiglass box filled with sediments and water that represents the shallow lagoon. This recipient was also subject to artificial lights to emulate the sun radiance. The plexiglass box has 48 x 75 x 48 cm^3 of height, length and width respectively, and was insulated with a $1\,cm$ thick polystyrene layer. A vertical high-resolution DTS system was constructed to simultaneously measure the thermal profile of the air, water, and sediments. The DTS system consists in a vertical pole, two water baths at different temperatures that are used for calibration purposes, and a fiber-optic cable that connects all the components of the DTS system. The vertical pole was installed at the center of the plexiglass box. It consists in, a $10\,cm$ diameter cylinder and filled with insulating foam. A $0.9\,mm$ simplex tight-buffered fiber-optic cable(AFL Telecommunications, Spartanburg, SC) was wrapped around the cylinder to obtain the vertical temperature profile in the system. This cable was connected to a Ultima-XT DTS instrument (Silixa, Herthfordshire, England). The total length of the fiber-optic cable was

$\sim 240\,m$, with $\sim 60\,m$ in each bath . Then, the box was filled with $25.5\,cm$ of organic soil of an artificial lake located near to the university campus, and with a water column that varies between 2 and $5.5\,cm$ of height. Over the box, at a distance of $10\,cm$ a set of two led lights were mounted, each one with a power of $\approx 400\,W$, resulting in $\approx 800\,W/m^2$ of direct heat net source to the system. This arrangement was adjusted to turned on and off periodically so that the period of both states were the same. The tested periods were 2, 4 y 6 hours.

3 Results

Figure 2 shows the dependency of the magnitude of the modal thermal amplitudes with the dimensionless numbers Π_1 and Π_2. The segmented line in Figure 2A represents the case when $k_t \to \infty$, when the turbulence in the water column is really important, implying that the water temperature is the same than of the WSI. The variable $|T_w^*|$ represents the module of the ratio between the thermal mode and the characteristic modal thermal amplitude $\widetilde{T_{w_m}}$. The circles in both plots of Figure 2 correspond to the values obtained with the TP-200 sensors, while the squares correspond to the measurements with the DTS system. When $\Pi_1 = 0$, there is no heat exchange between sediments and water, so that in the heat balance (1) H_g must be neglected and solved only considering the atmospheric forcing. This case happens when the water level or the forcing frequency are too high. On the other hand, when $\Pi_1 \to \infty$, the water level or the forcing frequency are very low (years or days). In this context, the dots in Figure 2A are below the limiting case when $h_t \to \infty$, having smaller thermal amplitudes than those that occur when the turbulent transport is really efficient. This values were obtained using the experimental water depth, forcing frequency, and an adjusted forcing so that the values of experimental T_{w_m} were the same than the theoretical ones obtained with (11). The value of k_t was obtained with the mean value of $k_t = \kappa_s(\rho c_p)_s \partial T_s/\partial z \cdot ((\rho c_p)_w(T_w - T_{WSI}))^{-1}$ for the TP-200 experiments, and the mean value of k_t from the log of δ_c as is shown in Figure 3B for the DTS ones. The Figure 2B shows the importance of Π_2. When $\Pi_2 = 0$, there is no heat exchange between the water and the sediments, since $k_t = 0$. In contrast, if $\Pi_2 \to \infty$, the turbulent transport is really efficient ($k_t \to \infty$), so the heat flux H_g is controlled by diffusive processes in the sediments. The thermal amplitudes obtained with the TP-200 experiments shows a good fit with the theoretical curve, while the DTS data does not fit so good. This could be because the value of k_t is not being well represented, as it can be a possible water stratification, or could be because the forcing H is not well parameterized. Further investigation is required to elucidate this response.

Figure 3 shows the time series of the net forcing estimated as a fraction of the forcing measured from the set of lamps, the time series for k_t and mean water temperature for a experiment with a period of $T = 6\,[hr]$, and a water height of $h = 3.5[cm]$. It can be seen that when the lamps are lighted on, the water responds and raises its temperature, reaching a maximum when the lights go out. The same occurs for k_t, which increases its value as the water temperature does. In contrast, when the lights are turned off, it can be seen a peak on the values of the mentioned variable (k_t). This behavior can be explained in the similarity of water and sediment temperatures, reaching a $\delta_c \approx 0$ so that when the relation κ_s/δ_c holds, these peaks appear. In this way, Figure 3(B) shows the variation of the dimensionless heat transfer coefficient $k_t^* = k_t h/\kappa_s$, obtained measuring the height of the diffusivity sublayer where the water temperature varies from

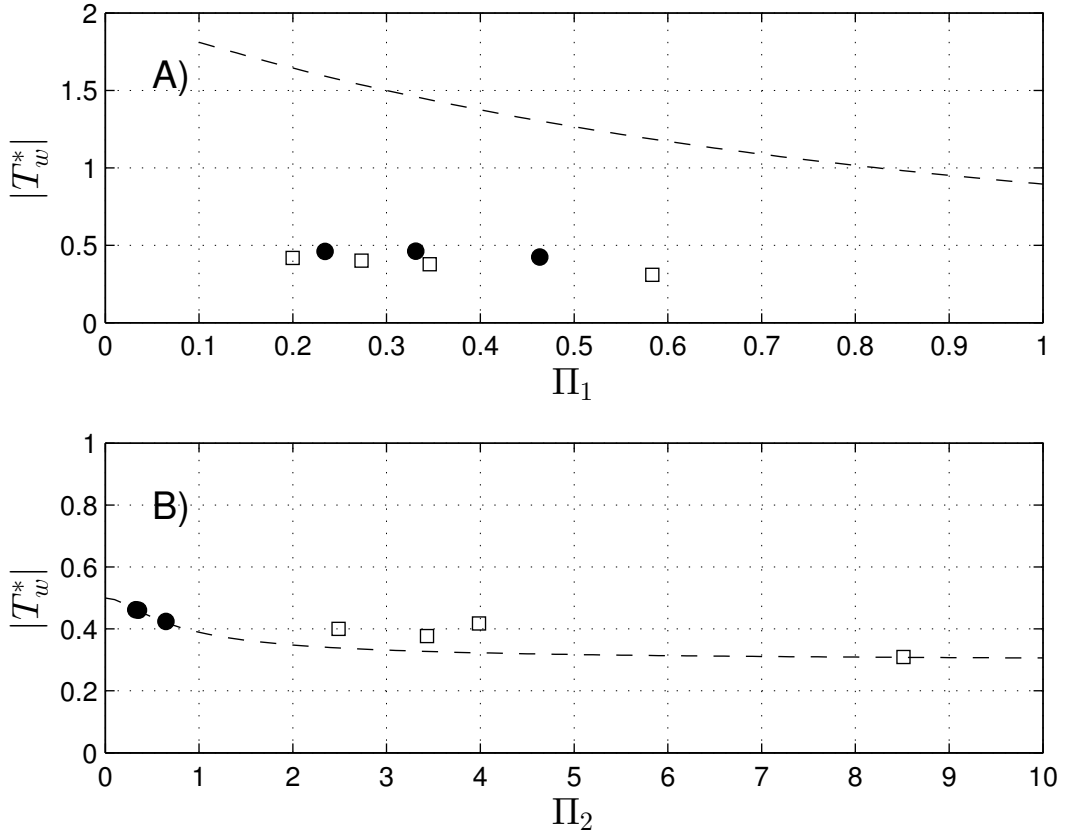

Figure 2: Influence of dimensionless numbers in the temperature modal amplitudes. Circles are TP-200 data and squares are DTS data. A) $|T_w^*|$ as a function of Π_1. The segmented line represents the case when $k_t \to \infty$. B) $|T_w^*|$ as a function of Π_2. The segmented line represents the theorical value of $|T_w^*|$ for different values of dimensionless Π_2.

the WSI to the mean value of T_w. Then a thermal diffusion coefficient was estimated considering a Prandtl of 7. A FFT was applied to the forcing series Figure 3A in order to obtain the values of H_m. As the frequency of each mode of H are known with this method, a series of the dimensionless numbers Π_1 and Π_2 can be obtained, using the mean value of k_t as a representative value of the experience. Using (11) a series of T_{w_m} were obtained and therefore, a theoretical variation of temperature in time (Figure 3C). From the experimental temperature variation can be observed that the decay and increase rate are not linear, which can been explained by changes in k_t, producing convective instabilities that are responsible of turbulent fluxes from the sediment to the atmosphere.

4 Conclusions and Discussion

In this paper we presented the preliminary experimental results of periodic heat exchanges between water and sediment in extremely shallow lakes. The results were analyzed in terms of 2 dimensionless numbers that quantify the importance of sediments (Π_1), and heat transfer velocity (Π_2) in the water temperature of shallow waters.

The dimensionless number Π_1 quantify the the influence of the sediment in the water heat balance, so that when it have small values, H_g can be neglected in (1) because its

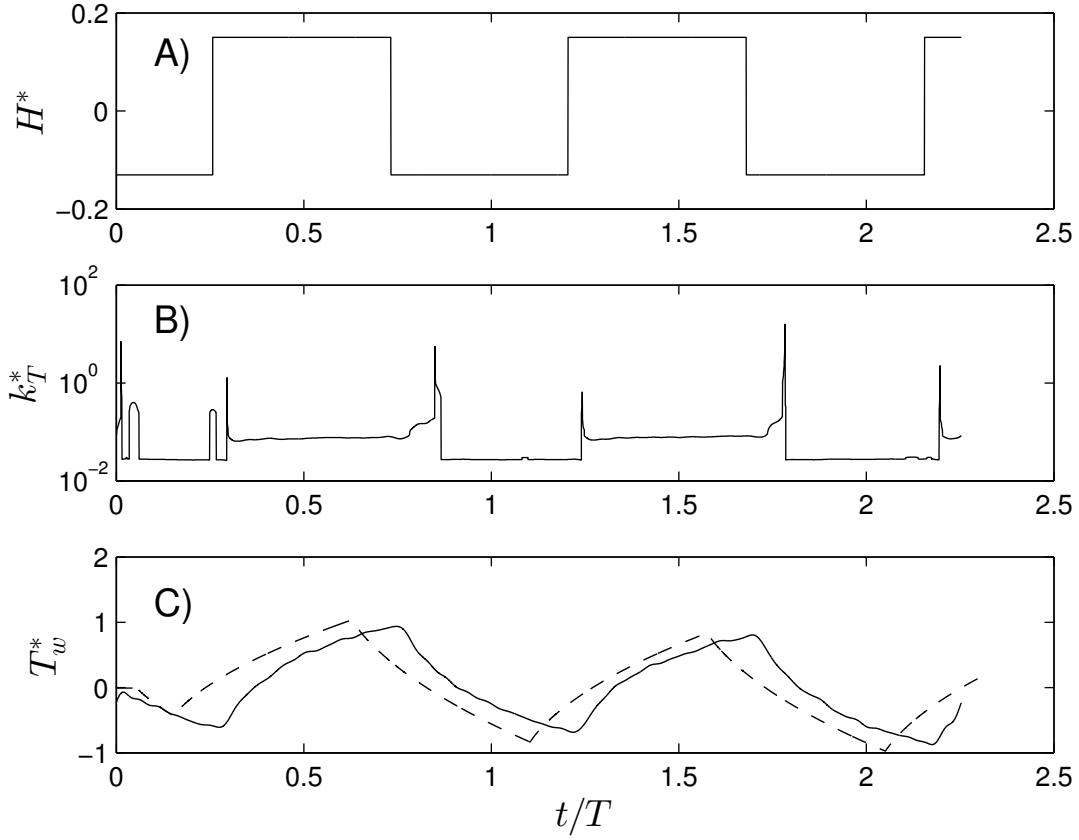

Figure 3: A)Times series of the net atmospheric forcing normalized by the max value of H B) Time series of k_t^*. C) Time series of the measured water temperature (cotinuous line) and theorical temperature(dashed line) obtained through Π_2 and Π_1.

contribution is very little. In contrast, for large values of Π_1 the heat balance is described by $H = H_g$. In other hand, Π_2 represents the relative importance of turbulence transport in the water column, because when it reach small values, the sediment act as a adiabatic boundary condition, so that much of the heat is retained in the water. The opposite happens when Π_2 reaches high values, due to heat transport in water column is very efficient so that $T_w = T_{WSI}$ and the heat transfer H_g is controlled by sediment.

Regarding to k_t, it can be seen that takes positive values when the temperature is rising (i.e., when the lights are on), favoring turbulent transport from the sediments to the water column. The dots of DTS experiments in Figure 2B showed that there is a noise source that is making the difference between the theoretical solution and the experimental results. The relationship $k_t = \kappa_s/\delta_c$ considered a permanent regime and a trickling flow in the section, conditions that are not present in the made experiences. Also, the used method considered the distance from the WSI to the condition when the mean water temperature are reached, so stratification in the water column could be making noise in the logged data. Other noise source may be the forcing source, because approximately a 15% of H is being used as a effective source of heating. In this way, more experiments should be conducted to characterize other atmospheric sources like latent heat, convective heat and long-wave radiance.

In Figure 2A the data resulted in lower modal temperatures than the theoretical case

when $k_t \to \infty$. This can be explained because in that case, the water temperature is almost or equal the sediment temperature, presenting no attenuation from the second one to the first one recently mentioned. Thus, the thermal amplitudes achieved in the water column are lower than the case when $T_w = T_{WSI}$ can be assumed, so that an important fraction of the heat are being stored in sediment.

References

Bachelor, G. (1967). *An introduction to fluid mechanics*.

Bogan, T., Mohseni, O., and Stefan, H. (2003). Stream temperature-equilibrium temperature relationship. *Water Resources Research*, 39:1245.

de A. de la Fuente. Niño, A. (2010). Temporal and spatial features of the thermohydrodynamics of shallow salty lagoons in northern chile. *Limnology and Oceanography*, 55(1):279–288.

de la Fuente, A. (2014). Heat and dissolved oxygen exchanges between the sediment and water column in a shallow salty lagoon. *Geophysical Research:Biogeosciences*, 119(4):596–613.

de la Fuente, A. and Meruane, C. (2016). Dimensionless numbers for classifying the thermo-dynamical regimes that determine water temperature in shallow lakes and wedlands. *Submitted to Environmental Fluid Mechanics*.

Fang, X. and Stefan, H. G. (1998). Temperature variability in lake sediments. *Water Resources Research*, 34:717–729.

Necati, O. (1977). *Basic Heat Transfer*. Ohio:McGraw-Hill.

Suárez, F., Aravena, J., Hausner, M., Childress, A., and Tyler, S. (2011). Assesment of a vertical high-resolution distributed-temperature-sensing system in a shallow thermohaline environment. *Hydrology and Earth System Sciences*, 15:1081–1093.